

SIMULATING THE INFLUENCE OF WAVE WHITECAPS ON SAR IMAGES

Eugenio Pugliese Carratelli ^(1,3), Bertrand Chapron ⁽²⁾, Fabio Dentale ⁽¹⁾, Ferdinando Reale ⁽¹⁾

⁽¹⁾ University of Salerno, Via Ponte Don Melillo 84084 Fisciano (SA) Italy; fdentale@unisa.it; freale@unisa.it

⁽²⁾ IFREMER, Laboratoire d'Océanographie Spatiale (LOS), Plouzané 29280 France; Bertrand.Chapron@ifremer.fr

⁽³⁾ CUGRI, Piazza Vittorio Emanuele 84084 Penta di Fisciano (SA) Italy; epc@unisa.it

ABSTRACT

This work provides a new application of numerical pseudo-random simulation of satellite active sensor imagery ([1] and [2]), which allows a greater freedom to introduce complex hydrodynamic mechanisms compared to the traditional spectral analytical procedure.

After previous works [3] and [4] on the basic methodology, which mainly concentrated on tilting and Doppler shift effects, the possibility is examined here of including the effects of wave whitecapping in the simulation. Recent results as in [5] and [6] highlight the importance of wave breaking and the consequent formation of whitecaps on the image formation mechanism. Such an effect was already considered in [7] and [8] in connection with passive microwave sensors; it was also taken into account as a possible element of SAR sea current visualization by [5], [6] and [9], but it is still relatively new within the context of SAR wind and wave analysis, which until recently was assumed to depend mainly on capillary wave modulation and tilt. On the other hand, in the last few years the understanding of offshore wave breaking and whitecap formation has improved to the point that such processes can be confidently included in the image modeling.

Some examples are given on how to represent whitecapping in the simulation, also by including the effects of the Doppler shift and its role in generating the final SAR image.

Results from [10] and [11] are used to identify the generation of whitecaps through an appropriate parameter, together with up to date formulas for the determination of whitecap covered sea surface fraction as exposed in [12] and [13]. Numerical spectral SAR images are simulated in previous works [3] and [4].

1. WHITECAP COVERED FRACTION

The formation of whitecaps on the sea surface is a long standing research subject. References [12], [13] and [14] provide an extensive reviews of results on the dependence of the whitecap covered sea surface fraction, here denoted as W , on measurable parameters such as wind speed, fetch, and sometimes wave age. In many situations (short fetches, unsteady winds) there seems to be a difficulty in determining the appropriate

parameters - probably because of the strong influence of the instantaneous and local wind speed on the whitecap formation, which cannot be reproduced by large scale wind and sea state parameters.

Some results however seem to be consistent enough for steady seas and long fetches as shown by Eqs. 1 and 2 already proposed in [12]:

$$W(\%) = 0.06 C_D U_{10}^{7/3} X^{0.33} \quad (1)$$

$$C_D = \frac{k^2}{[12.505 + 0.358 \ln(X) - 2.716 \ln(U_{10})]^2} \quad (2)$$

Here k is a constant (assumed to be $k = 0.4$), X the fetch and U_{10} the wind speed at a height of 10 meters.

Obviously whitecapping is only one of the Radar Cross Section formation mechanisms; assuming as in [6] (see Eq. 3)

$$\sigma_o = \sigma_{oc}(1 - W) + \sigma_{ob}W \quad (3)$$

that averaged (over many wavelengths) radar cross section σ_o to be given by the sum of a "Braggs" capillary wave component σ_{oc} (where the surface is not covered by foam) and σ_{ob} (over the broken wave fraction), it is possible to reproduce CMOD-4 with three parameters; if for instance σ_{oc} is taken as in Eq. 4, the result is given by Eq. 5.

$$\sigma_{oc} = bU_{10}^m \quad (4)$$

$$\sigma_o = bU_{10}^m(1 - W) + \sigma_{ob}W \quad (5)$$

Fig. 1 shows the results taken by combing CMOD-4 model and Eq. 5.

Some results should not induce too much confidence, and indeed, for one thing, CMOD-4 is only acceptable for winds below $20 - 25 \text{ ms}^{-1}$. However comparing Eq. 5 with more advanced results could provide some understanding on the backscattering behaviour of both capillary waves and foam.

Simulating SAR image formation is of course a much more complex task, which involves the necessity to determine the geometrical position of the whitecaps and

their velocity in order to take into account the Doppler shift effect.

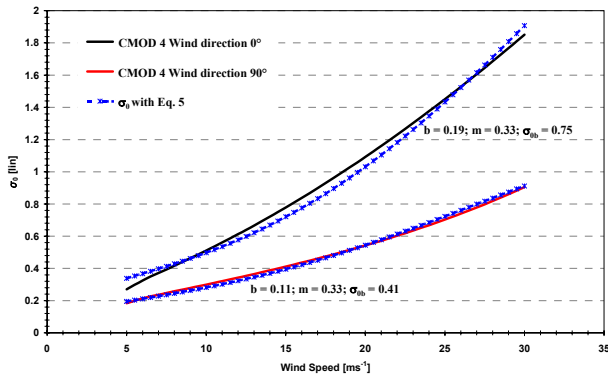


Figure 1. CMOD-4 Radar Equivalent Cross Section for $\theta = 23^\circ$; wind direction 0° and 90° . Eq. 5 for range travelling waves ($b=0.19$, $m=0.33$, $\sigma_{ob}=0.75$) and for azimuth travelling waves ($b=0.11$, $m=0.33$; $\sigma_{ob}=0.41$).

2. WHITECAP LOCATION

References [10] and [11] have provided extensive results of both laboratory and field work on the formation of whitecaps on the sea surface. Reference [10], in particular examine a number of local parameters which might provide an indication of wave breaking and therefore of whitecap coverage. Purely geometrical (surface curvature) or kinematic (velocity) based indicators are discarded in favour of the so called “dynamic indicator” a/g , based on the value a of the vertical acceleration of the surface particles (here g is the acceleration of gravity). Negative (i.e. downward) values of ratio a/g below a certain threshold are likely to induce wave breaking and therefore whitecapping.

Such a parameter is easy to calculate with a numerical spectrum based simulation technique such as outlined in [15] and described in detail in [16]. Local vertical acceleration component are calculated for each pixel (1m x 1m in all the cases shown) and, once a threshold is decided, pixels below such a threshold are assumed to be covered by foam. Fig. 2 shows a two dimensional example of model implementation here described.

It goes without saying that there are a number of caveats to take into account before this method can be employed with full confidence: in particular – even assuming the validity of the dynamic parameter as a wave breaking trigger – the foam generated during the wave breaking stays afloat for a considerable time after the actual whitecap formation event, and its thickness could also play a role in microwave scattering such as it does in emissivity. A more complete procedure based on tracking the foam path could be produced by following the floating pollutant approach as in [16], but this effect is not included yet in the model presented here.

Given all this, setting the downward acceleration threshold is no trivial task. A possible procedure is outlined in the following.

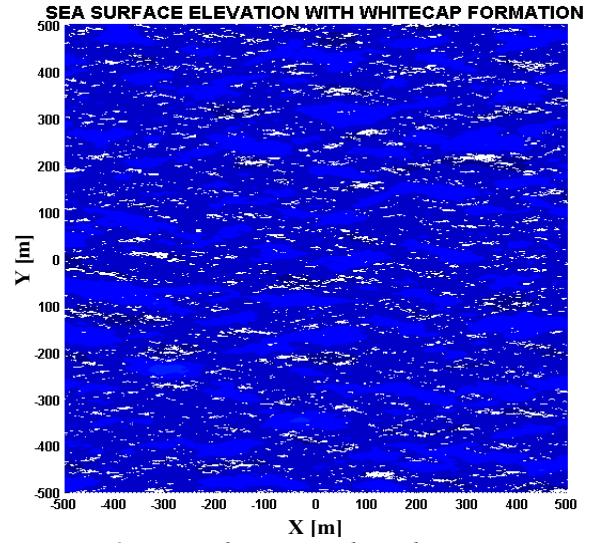


Figure 2. Water elevation and acceleration map - Simulated whitecaps are marked in white.

In the first place the empirical frequency distribution and cumulate functions F of the acceleration values are computed from the wave field numerical simulation results.

The fraction F is then set at the appropriate W value, such as might be supplied by Eqs. 1 and 2 reported above, or by similar empirical models. In this case it is assumed $W = F = 5\%$ which corresponds to a breaking threshold value for the acceleration a of about -2 ms^{-2} (Fig. 3).

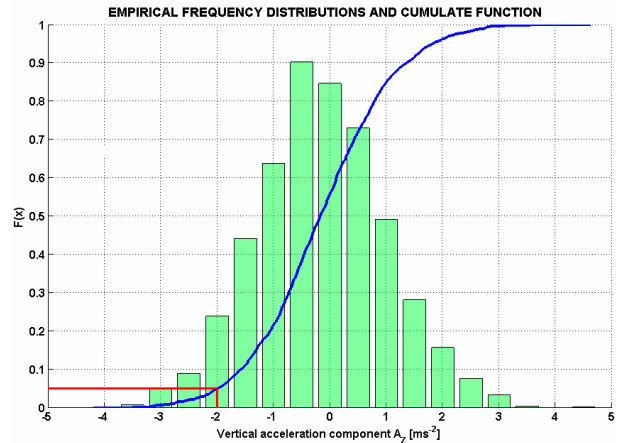


Figure 3. Vertical acceleration distribution and cumulate function.

A one-dimensional application of this procedure is shown in Fig. 4.

It is worth noting that this procedure – linking whitecaps formation with downward acceleration and then indirectly with water heights– might also eventually supply a key to locate the highest peaks from radar images.

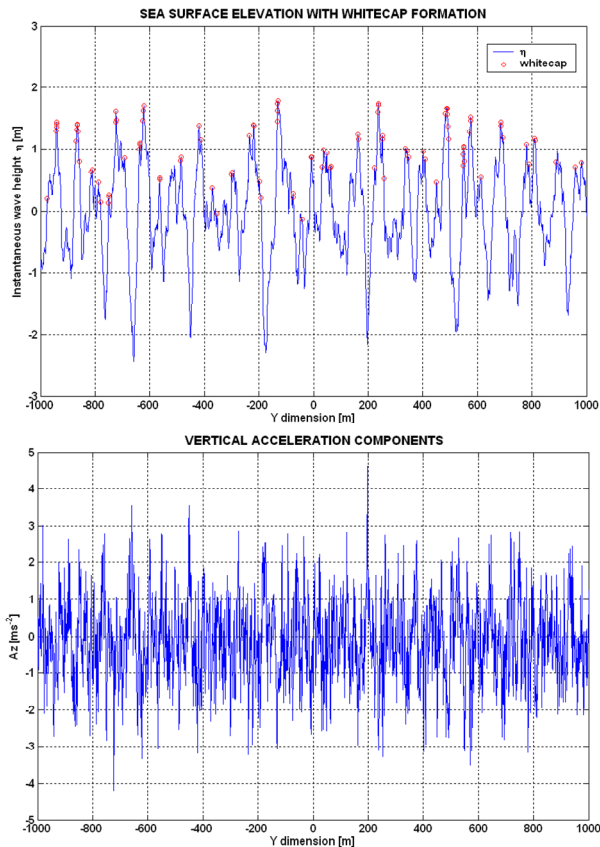


Figure 4. Water elevation and acceleration map. Simulated whitecaps are marked with red circles.

3. SAR WHITECAP IMAGE SIMULATION

As stated above, the (real aperture) radar cross section distribution of a wave field - very much like its averaged value - derives from the capillary wave Bragg backscattering, which interacts with the water surface tilt and the orbital velocity (“hydrodynamic modulation”), combined with the whitecapping effect. Numerical simulation of the former was described in previous work; the treatment of the latter is briefly outlined in the following.

Whitecaps backscattering is here assumed to be Lambertian, i.e. independent from tilt and from the look angle, so that pixel are given a fixed value, i.e. 1 if breaking occurs according to the previous criterion, or 0 if it does not.

Under these assumptions, an RAR high resolution (1m) image of a strictly one-directional sea would therefore look like a succession of random white and black stripes, as shown in Fig. 5a.

Under the current assumption, it would make no difference whether the sea is azimuth or range directed. For an azimuth propagating sea, however, the distribution of such stripes would change according to the SAR Doppler effect, which can be easily taken into account by numerical simulation as in [3] and [4] (Fig. 5b). Its effects is a mere scrambling of the lines;

obviously velocity bunching does not play here a critical role in making the wave field visible. The images above, however, were simulated with a resolution much higher (1 pixel = 1m x 1m) than that of the current satellite SAR; introducing a realistic radar image resolution, much lower than the typical size of the whitecaps – or in the simulation, than the computational pixel size – the image would then look like a succession of grey shaded lines as Fig. 6 shows.

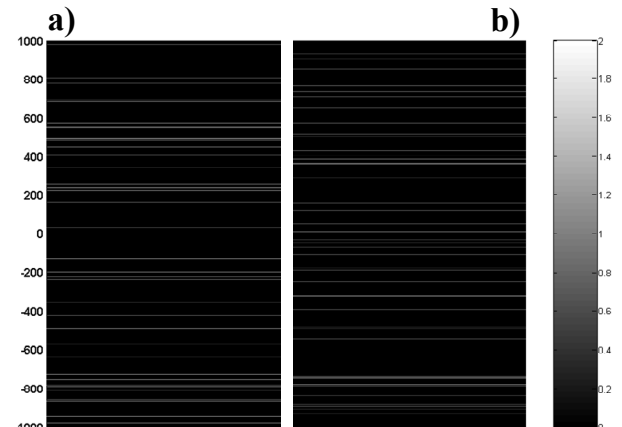


Figure 5. a) RAR whitecap effect resolution 1m; b) SAR whitecap effect resolution 1m.

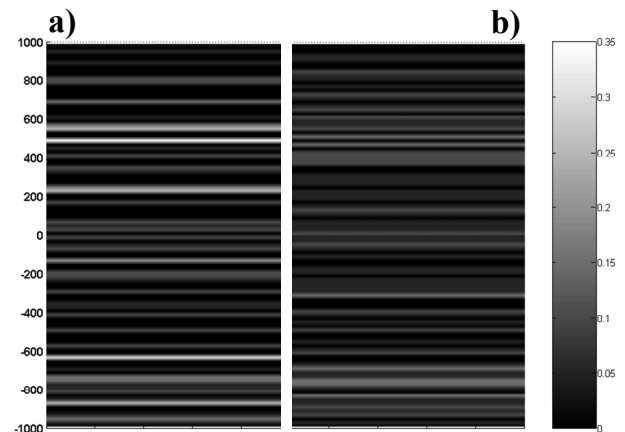


Figure 6. a) RAR whitecap effect resolution 20m; b) SAR whitecap effect resolution 20 m.

4. CONCLUSIONS

Whitecap formation and spatial distribution has been considered in connection with numerical spectral pseudo-random simulation. Wave breaking local threshold parameters related to geometric, kinematic and dynamic breaking criteria can indeed be much more exactly computed on the basis of a numerical realization than with a purely analytical spectral approach.

An example of SAR image simulation has been presented here for a very simple case, which can be extended to include other aspects of the whitecap formation and of the foam movement over the sea

surface, as well as more complex hypotheses on its backscattering behaviour.

It has been shown that all the sea surface hydrodynamic mechanisms can effectively be included within the numerical spectral pseudo-random simulation, thus providing a useful tool to a better understanding of SAR sea wave image formation.

5. ACKNOWLEDGEMENTS

Some of the data used for this work were provided through ESA-ESRIN Project CAT-1 No 1172: "Remote sensing of wave transformation"; the authors are grateful to Dr. Jerome Benveniste (Esa – Esrin) for help and support.

6. REFERENCES

1. Brüning, C., Alpers, W. & Hasselmann, K. (1990). Monte Carlo Simulation studies of the nonlinear imaging of a two dimensional surface wave field by a synthetic aperture radar. *International Journal of remote Sensing* **11**(10), 1695-1727.
2. Della Rocca, M.R. & Pugliese Carratelli, E. (2000). A model for Wind Speed and Wave Height Retrieval from Radar Altimeter Measurements. *ERS ENVISAT Symposium – Gothenburg* –Sweden 16-20
3. Pugliese Carratelli, E., Dentale, F. & Reale, F. (2006). Numerical Pseudo-Random Simulation of SAR Sea and Wind Response. In *Proc. of SEASAR 2006, 23-26 January 2006, Frascati, Italy 'Advances in SAR Oceanography from Envisat and ERS Missions'* (Ed. H. Lacoste), ESA SP-613 (CD-ROM), ESA Publications Division, European Space Agency, Noordwijk, The Netherlands.
4. Pugliese Carratelli, E., Dentale, F. & Reale, F. (2007). Reconstruction of SAR Wave Image Effects through Pseudo Random Simulation. In *Proc. of the Envisat Symposium 2007, 23-27 April 2007, Montreux, Switzerland* (Eds. H. Lacoste & L. Ouwehand), ESA SP-636 (CD-ROM), ESA Communication Production Office, European Space Agency, Noordwijk, The Netherlands.
5. Kudryavtsev, V., Hauser, D., Caudal, G. & Chapron, B. (2003a). A semiempirical model of the normalized radar cross-section of the sea surface 1. Background model. *Journal of Geophysical Research* **108**(C3).
6. Kudryavtsev, V., Hauser, D., Caudal, G. & Chapron, B. (2003b). A semiempirical model of the normalized radar cross-section of the sea surface 2. Radar modulation transfer function. *Journal of Geophysical Research* **108**(C3).
7. Kerbaol, V. (1997). Analyse spectrale et statistique vent-vagues des images radar à ouverture synthétique. *These de docteur. Université de Renne I*.
8. Reul, N. & Chapron, B. (2003). A model of sea-foam thickness distribution for passive microwave remote sensing applications. *Journal of Geophysical Research* **108**(C10).
9. Johannessen, J.A., Kudryavtsev, V., Akimov, D., Eldevik, T., Winther, N. & Chapron, B. (2005). On radar imaging of current features: 2. Mesoscale eddy and current front detection, *Journal of Geophysical Research* **110**(C07017).
10. Oh, S.-H., Mizutani, N., Suh, K.-D. & Hashimoto, N. (2005). Experimental investigation of breaking criteria of deepwater wind waves under strong wind action. *Applied Ocean Research*. **27**(2005), 235-250.
11. Sugihara, Y., Tsumori, H., Yoshioka, H., Serizawa, S. & Masuda, A. (2004). Imaging Measurement of Whitecaps at Sea Observation Tower. *Proceedings of the 29th International Coastal Engineering Conference*. Lisbon, Portugal, 19 – 24 September.
12. Piazzola, J., Forget, P. & Despiau, S. (2002). A sea spray generation function for fetch-limited conditions. *Annales Geophysicae* **20**, 121–131. European Geophysical Society.
13. Lafon, C., Piazzola, J, Forget, P. & Despiau, S. (2005). Modelling of whitecap coverage in coastal environment. *37th International Liège Colloquium on Ocean Dynamics, Gas Transfer at Water Surfaces*.
14. Melville, W.K. & Matusov, P.R. (2002). Distribution of breaking waves at the ocean surface. *Letters to Nature*.
15. Pugliese Carratelli, E., Giarrusso, C. & Spulsi, G. (2005). Analisi delle immagini da SAR satellitare sul mare. *26° Corso Di Aggiornamento in Tecniche per la Difesa dall'Inquinamento*, Guardia Piemontese, Italy (In Italian).
16. Giarrusso, C.C., Pugliese Carratelli, E. & Spulsi, G. (2001). On the Effects of Wave Drift on the Dispersion of Floating Pollutants. *Ocean Engineering* **28**(10), 1339-1348.